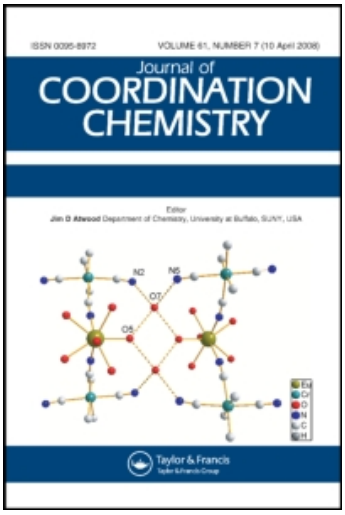

Journal of Coordination Chemistry
Publication details, including instructions for authors and subscription information:
http://www.informaworld.com/smpp/title~content=t713455674

HETERO-ALKOXIDE GROUP (IV) AND (V) NEO-PENTOXIDE COMPOUNDS. SYNTHESES, CHARACTERIZATIONS, AND X-RAY STRUCTURES OF $[Zr(\mu\text{-}OCHMe_2)(OCH_2CMe_3)_3(HOCH_2CMe_3)]_2$ AND $[Ta(\mu\text{-}OCH_2Me)(OCH_2CMe_3)_4]_2$

Timothy J. Boyle[a]; Jesus J. Gallegos III[a]; Dawn M. Pedrotty[a]; Eric R. Mechenbier[a]; Brian L. Scott[b]
[a] Sandia National Laboratories, Advanced Materials Laboratory, 1001 University Boulevard SE, Albuquerque, NM, USA [b] Los Alamos National Laboratories, CST-18, Chemical Science and Technology Division -X-ray Diffraction Laboratory, Los Alamos, NM, USA

To cite this Article Boyle, Timothy J. , Gallegos III, Jesus J. , Pedrotty, Dawn M. , Mechenbier, Eric R. and Scott, Brian L.(1999) 'HETERO-ALKOXIDE GROUP (IV) AND (V) NEO-PENTOXIDE COMPOUNDS. SYNTHESES, CHARACTERIZATIONS, AND X-RAY STRUCTURES OF $[Zr(\mu\text{-}OCHMe_2)(OCH_2CMe_3)_3(HOCH_2CMe_3)]_2$ AND $[Ta(\mu\text{-}OCH_2Me)(OCH_2CMe_3)_4]_2$', Journal of Coordination Chemistry, 47: 1, 155 — 171
To link to this Article: DOI: 10.1080/00958979908024550
URL: http://dx.doi.org/10.1080/00958979908024550

J. Coord. Chem., 1999, Vol. 47, pp. 155–171
Reprints available directly from the publisher
Photocopying permitted by license only

HETERO-ALKOXIDE GROUP (IV) AND (V) NEO-PENTOXIDE COMPOUNDS. SYNTHESES, CHARACTERIZATIONS, AND X-RAY STRUCTURES OF $[Zr(\mu\text{-}OCHMe_2)(OCH_2CMe_3)_3(HOCH_2CMe_3)]_2$ AND $[Ta(\mu\text{-}OCH_2Me)(OCH_2CMe_3)_4]_2$

TIMOTHY J. BOYLE[a,*], JESUS J. GALLEGOS III[a], DAWN M. PEDROTTY[a], ERIC R. MECHENBIER[a] and BRIAN L. SCOTT[b]

[a]*Sandia National Laboratories, Advanced Materials Laboratory, 1001 University Boulevard SE, Albuquerque, NM 87106, USA;* [b]*Los Alamos National Laboratories, CST-18, Chemical Science and Technology Division – X-ray Diffraction Laboratory, Los Alamos, NM 87545, USA*

(Received 15 January 1998; Revised 15 May 1998; In final form 29 June 1998)

The alcoholysis exchange between excess HONp and $[Zr(OPr^i)_4(HOPr^i)]_2$ or "$Ta(OEt)_5$" led to isolation of the mixed-alkoxide compounds $[Zr(\mu\text{-}OPr^i)(ONp)_3(HONp)]_2$ (**1**) and $[Ta(\mu\text{-}OEt)(ONp)_4]_2$ (**2**), respectively. Compounds **1** and **2** were found to adopt an edge-shared bioctahedral geometry, $[M(\mu\text{-}OR')(OR)_5]_2$, with the smaller ligands acting as the bridge between the two metal centers. For **1**, the octahedral geometry around the metal center is completed by the coordination of a HONp solvent molecule. The solid state structure of **1** was retained in saturated solutions but at lower concentrations, dynamic behavior associated with a mononuclear–dinuclear equilibrium was observed. For **2**, at low concentrations an equilibrium between mononuclear and dinuclear complexes was noted; however, at higher concentrations a dinuclear-higher-nuclearity equilibrium was noted.

Keywords: Metal alkoxides; metal-alkoxide ceramics; zirconium; tantulam; X-ray structures

* Corresponding author. E-mail: tjboyle@sandia.gov.

INTRODUCTION

Metal alkoxides are of great interest as precursors to metal oxide ceramics.[1-7] To control and optimize the properties of the resulting materials, it is necessary to know the identity of the starting precursors both in solution and solid state; however, few reports detail the actual structural characterization of "simple" Group (IV) or (V) metal-alkoxide compounds.[1-5,8-19] This is typically due to the fact that the starting materials exist as oils or are poorly soluble in standard solvents.

The neo-pentoxide ligand ($OCH_2CMe_3 = ONp$) is extremely attractive for material applications due to the β-hydrogen (critical for uniform materials production upon exposure to atmospheric moisture) and the *tert*-butyl moiety, which simultaneously increases solubility and reduces oligomerization. We have recently reported the synthesis and characterization of two unique metal neo-pentoxides: $[Ti(\mu\text{-}ONp)(ONp)_3]_2$[12] and $[Nb(\mu\text{-}OEt)(ONp)_4]_2$ ($OEt = OCH_2CH_3$)[13](see Figure 1). $[Ti(\mu\text{-}ONp)(ONp)_3]_2$ was synthesized through an alcoholysis exchange reaction between $Ti(OPr^i)_4$ ($OPr^i = OCHMe_2$) and HONp that resulted in complete exchange of the OPr^i ligands (Equation (1)),[12] however, the reaction between "$Nb(OEt)_5$" and HONp resulted in the mixed ligated species $[Nb(\mu\text{-}OEt)(ONp)_4]_2$ (Equation (2)):[13]

$$2Ti(OPr^i)_4 + 9HONp \xrightarrow[-8HOPr^i]{tol/\Delta} [Ti(\mu\text{-}ONp)(ONp)_3]_2 \qquad (1)$$

$$2\text{“}Nb(OEt)_5\text{”} + 11HONp \xrightarrow[-8HOEt]{tol/\Delta} [Nb(\mu\text{-}OEt)(ONp)_4]_2 \qquad (2)$$

Both of these compounds were used for the production of ferroelectric thin films.[6,7,13] Therefore, we were motivated to characterize other early transition metal ONp derivatives.

Due to the dearth of well-characterized homonuclear metal alkoxides and the inconsistency of complete alcohol exchange, structural characterizations of the resultant products were realized through X-ray crystallographic investigations. In this paper we report the syntheses and characterizations (solid and solution state) of $[Zr(\mu\text{-}OPr^i)(ONp)_3(HONp)]_2$ (**1**, Figure 2) and $[Ta(\mu\text{-}OEt)(ONp)_4]_2$ (**2**, Figure 3). Solution studies using NMR spectroscopy were also undertaken to elucidate the solution behavior of these compounds. A comparison of the Group (IV) and (V) congeners' characteristics were explored to derive general properties of these novel mixed-alkoxide compounds.

EXPERIMENTAL SECTION

All compounds were handled under an inert atmosphere using standard Schlenk and glove box techniques, unless otherwise noted. All solvents were freshly distilled and dried according to literature procedures.[15] FT-IR data were obtained on a Nicolet, Magna System Spectrometer-550. Elemental analyses were performed on a Perkin-Elmer 2400 CHN-S/O Elemental Analyzer. Solution state NMR and variable temperature NMR spectra were obtained using a 5 mm BB solution probe on an AMX 400 spectrometer: ^{1}H (400.1 MHz), ^{13}C (100.6 MHz). All spectra were referenced against the residual proton impurity in the appropriate dried deuterated solvent. The following compounds were used as received (Aldrich): HONp, $[Zr(OPr^i)_4(HOPr^i)]_2$, and "$Ta(OEt)_5$".

$[Zr(\mu\text{-}OPr^i)(ONp)_3(HONp)]_2$, 1

HONp (0.63 g, 7.09 mmol) was added *via* an addition funnel to a stirred solution of $[Zr(OPr^i)_4(HOPr^i)]_2$ (0.50 g, 1.29 mol) in toluene (~12 mL). The reaction mixture was heated between 60° and 90°C for 12 h, followed by removal of the volatile material *in vacuo* to yield an off-white powder. After several days, the cooled (−35°C) concentrated toluene extract yielded crystals (81.0% yield, 0.52 g) which proved to be **1**. ^{1}H NMR (C_6D_6, 400.1 MHz, saturated solution): δ 4.66 (1.0H, sept., $OCHMe_2$, J_{H-H} = 6.0 Hz), 3.88 (5.3H, s, OCH_2CMe_3), 1.42 (7.5H, d, $OCHMe_2$, J_{H-H} = 6.4 Hz), 1.06 (23.6H, s, OCH_2CMe_3). ^{13}C{H}NMR (C_6D_6, 100.6 MHz, saturated solution): δ 79.8 (OCH_2CMe_3), 71.0 ($OCHMe_2$), 33.9 (OCH_2CMe_3), 27.3 (OCH_2CMe_3), 26.8 ($OCHMe_2$). FT-IR (KBr pellet): 2952 (w), 2866 (w), 2693 (w), 1481 (br, m), 1394 (m), 1361 (m), 1261 (m), 1136 (s, br), 1030 (s), 944 (m), 904 (w), 824 (m), 751 (w), 632 (m, br), 566 (m), 466 (m) cm^{-1}. Elemental analysis calculated for $C_{46}H_{102}O_{10}Zr_2$: Theoretical: C, 55.37%; H, 10.30%. Found: C, 55.90%; H, 9.97%.

$[Ta(\mu\text{-}OEt)(ONp)_4]_2$, 2

HONp (3.57 g, 40.6 mmol) was added *via* an addition funnel to a stirred solution of "$Ta(OEt)_5$" (3.00 g, 7.39 mmol) in toluene (~100 mL). The reaction mixture was stirred in an oil bath at 60–90°C for 12 h followed by removal of the volatile material *in vacuo*. The resulting white powder was washed several times with hexanes, followed by extraction with hot toluene. Upon cooling, X-ray quality crystals were isolated (3.69 g; 79.0% yield)

which proved to be **2**. ^{1}H NMR (400.1 MHz, toluene-d_8, saturated solution): δ 3.41(4.8H, br mult., OCH_2Me), 3.08 (10.6H, s, OCH_2CMe_3), 1.02 (70.5H, br mult., OCH_2Me), 0.81 (70.5H, s, OCH_2CMe_3). $^{13}C\{^{1}H\}$ NMR (100.6 MHz, toluene-d_8, saturated solution): δ 73.6 (OCH_2CMe_3), 58.5 (OCH_2Me), 33.2 (OCH_2CMe_3), 26.7 (OCH_2CMe), 19.0 (OCH_2Me). FT-IR (KBr pellet): 2953 (br, w), 2983 (br, w), 2866 (br, w), 2740 (w), 2701 (w), 1481 (s), 1395 (s), 1361 (s), 1295 (w), 1262 (w), 1162 (sh), 1096 (br, s), 1023 (s), 937 (w), 904 (w), 877 (m), 751 (w), 685 (s), 661 (m), 649 (s), 506 (m), 446 (w) cm^{-1}. Elemental analysis calculated for $C_{44}H_{98}O_{10}Ta_2$: Theoretical: C, 45.99%; H, 8.59%. Found: C, 45.96%; H, 8.29%.

X-ray Collection, Structure Determination, and Refinement

Compounds **1** and **2** were handled in a pool of mineral oil under an argon gas flow. A crystal was attached to a thin glass fiber using silicon grease and then placed under a liquid nitrogen stream on a Siemens P4/PC diffractometer. The radiation used was graphite monochromatized MoKα: ($\lambda = 0.71069$ Å). The lattice parameters were optimized from a least-squares calculation on 25 carefully centered reflections of high Bragg angle. The data were collected using ω scans with a 1.02° and 1.04° scan range for **1** and **2**, respectively. Three check reflections monitored every 97 reflections showed no systematic variation of intensities. Lattice determination and data collection were carried out using XSCANS Version 2.10b software. All data reduction, including Lorentz and polarization corrections, structure solution, and graphics were performed using SHELXTL PC Version 4.2/360 software. The structure refinement was performed using SHELX 93 software.[20] The data for compound **1** were not corrected for absorption due to the low absorption coefficient. The data for compound **2** were corrected for absorption using the ellipsoid option in XEMP (SHELXTL PC). Table I lists the data collection parameters for **1** and **2**.

The structure of **1** was solved in the space group C2/c using direct methods and difference Fourier techniques. This solution yielded the zirconium and the majority of all other non-hydrogen atom positions. Subsequent Fourier synthesis gave all remaining non-hydrogen atom positions. One of the *tert*-butyl groups (atoms C9, C10, C10A, C10E and C10C) and the bridging iso-propoxide groups were modeled with a two-fold disorder. The site occupancy of the two components were fixed to one. All hydrogen atoms were fixed in positions of ideal geometry, with a C–H distance of 0.96 Å for methyl, 0.97 Å for methylene, and 0.98 Å for methine hydrogens and refined using the riding model in the HFIX facility in SHELXL 93.

These idealized hydrogen atoms had their isotropic temperature factors fixed at 1.2 (methylene and methine) or 1.5 (methyl) times the equivalent isotropic U of the carbon atom they were bonded to. Hydrogen atoms were not placed on the disordered *tert*-butyl group or on the minor methine carbon atom (C1A) of the disordered isopropyl group. All non-hydrogen atoms, except for C1A, were refined anisotropically. The final refinement converged to $R1 = 0.0813$ and $R2_w = 0.2111$.

The structure of **2** was solved in the space group $P\bar{1}$ using Patterson and difference Fourier techniques. This solution yielded the tantalum and oxygen atom positions. Subsequent Fourier synthesis gave all remaining non-hydrogen atom positions. All hydrogen atoms were fixed in positions of ideal geometry, with a C–H distance of 0.96 Å for methyl and 0.97 Å for methylene hydrogen atoms and refined using the riding model in the HFIX facility in SHELXL 93. These idealized hydrogen atoms had their isotropic temperature factors fixed at 1.5 times (methyl) or 1.2 times (methylene) the equivalent isotropic U of the carbon atom they were bonded to. The carbon atoms of the ethoxide ligands were modeled with a two-fold disorder. In addition, a few of the neo-pentoxide ligand methyl groups were also modeled with a two-fold disorder. No hydrogen atoms were placed on the disordered carbon atoms. The final refinement included anisotropic thermal parameters on all non-hydrogen atoms and converged to $R1 = 0.0334$ and $R2_w = 0.0868$.

RESULTS AND DISCUSSION

Due to the widespread use of metal alkoxides in materials production,[1–7] recent work in our laboratory has focused on the isolation, characterization, and implementation of novel precursors into material processes.[6,7,12,13,15,21,22] The neo-pentoxide derivatives for Ti and Nb were isolated from alcoholysis exchange reaction pathways (Equations (1) and (2)) as $[Ti(\mu\text{-}ONp)(ONp)_3]_2$[12] and $[Nb(\mu\text{-}OEt)(ONp)_4]_2$.[13] $[Ti(\mu\text{-}ONp)(ONp)_3]_2$ was synthesized in high yield as the trigonal-bipyramidal dinuclear complex (Figure 1(a)) and proved to be mononuclear in solution.[12] $[Nb(\mu\text{-}OEt)(ONp)_4]_2$ was isolated in moderate yield as the octahedral dinuclear complex (Figure 1(b)) and demonstrated a great deal of multi-nuclear dynamic behavior as evidenced by its ^{93}Nb NMR spectrum.[13] Due to the successful characterization and implementation of these compounds,[6,13] synthesis of their congeners were undertaken.

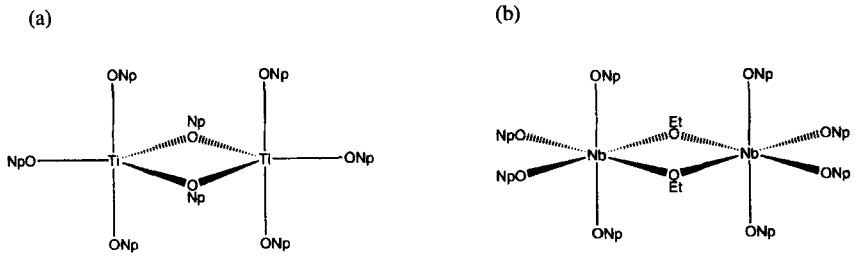

FIGURE 1 Schematic drawing of (a) $[Ti(\mu\text{-}ONp)(ONp)_3]_2$ and (b) $[Nb(\mu\text{-}OEt)(ONp)_4]_2$.

Synthesis

In an attempt to generate the Zr analog of $[Ti(\mu\text{-}ONp)(ONp)_3]_2$, $[Zr(OPr^i)_4(HOPr^i)]_2$ was dissolved in toluene and excess HONp was added *via* an addition funnel. There was no observable change in color or clarity of the solution after heating for 12 h at 60–90°C. The reaction mixture was cooled to room temperature and was then dried *in vacuo*. The resulting white powder was redissolved in toluene and cooled to −35°C which yielded crystals of $[Zr(\mu\text{-}OPr^i)(ONp)_3(HONp)]_2$, **1**:

$$[Zr(\mu\text{-}OPr^i)(OPr^i)_3(HOPr^i)]_2 + 11HONp \xrightarrow[-8HOPr^i]{tol/\Delta} [Zr(\mu\text{-}OPr^i)(ONp)_3(HONp)]_2 \quad (3)$$

Surprisingly, **1** was found to be significantly more soluble in C_6D_6 than in toluene-d_8.[23] It is also of note that **1** was readily soluble in hexanes, whereas, the parent alkoxide was not appreciably soluble at the same level. **1** was easily sublimed at temperatures < 150°C at 10^{-3} torr with no decomposition. Elemental analysis of the bulk sample of **1** proved to be consistent with the crystal structure when great care was taken to eliminate moisture and maintain the labile alcohol (the coordination of labile alcohols has been previously discussed for the OPr^i derivative).[9] Analyses of extensively washed and dried powders were consistent with "$Zr(\mu\text{-}OPr^i)(ONp)_3$".

A similar strategy was used to synthesize the tantalum ONp derivative, wherein HONp was added to "$Ta(OEt)_5$" in toluene. After stirring for 12 h at elevated temperatures, the volatile materials were removed *in vacuo*. The resultant powder was washed with hexanes and extracted with hot toluene. Upon cooling, crystalline material was isolated and proved to be

$[Ta(\mu OEt)(ONp)_4]_2$, **2**:

$$2\text{“}Ta(OEt)_5\text{”} + 11HONp \xrightarrow[-8HOEt]{tol/\Delta} [Ta(\mu\text{-}OEt)(ONp)_4]_2 \qquad (4)$$

2 was found to be poorly soluble in common organic solvents[24] but readily sublimed at temperatures around 180°C (at 10^{-3} torr). Elemental analysis of the bulk sample proved to be consistent with the solid state structure.

It appears that under these conditions the solution molecular complexity (MC) of the parent alkoxide dictates whether or not full exchange for the ONp ligands will occur. The homoleptic species, $[Ti(\mu\text{-}ONp)(ONp)_3]_2$, was formed from “$Ti(OPr^i)_4$” which has a reported MC = 1.4 in solution.[12] The isolation of $[Nb(\mu\text{-}OEt)(ONp)_4]_2$, **1**, and **2** indicates that in solution the reported dinuclear precursors [“$Nb(OEt)_5$”, $[Zr(OPr^i)_4(HOPr^i)]_2$, and “$Ta(OEt)_5$”][5] do not have their central core disrupted by introduction of the HONp at elevated temperatures. The general trend observed for the sublimation temperature volatility of the Group (IV) and (V) ONp compounds was $[Ti(\mu\text{-}ONp)(ONp)_3]_2$ (80°C) < $[Nb(\mu\text{-}OEt)(ONp)_4]_2$ (100°C) < **1** (150°C) < **2** (180°C) (*note*: attempts to sublime the OPr^i analog under identical conditions were not successful). The solubility of these compounds in toluene or hexanes follows the trend where $[Ti(\mu\text{-}ONp)(ONp)_3]_2 > \mathbf{1} > [Zr(OPr^i)_4(HOPr^i)]_2 > \mathbf{2} \approx [Nb(\mu\text{-}OEt)(ONp)_4]_2$. The formation of a mononuclear complex in solution would account for the high solubility of $[Ti(\mu\text{-}ONp)(ONp)_3]_2$; whereas, the weakly coordinated alcohol appears to increase the solubility of **1** and $[Zr(OPr^i)_4(HOPr^i)]_2$.

Solid State

Few of the proposed structures of the homo- and hetero-ligated alkoxy Group (IV) and (V) compounds have been crystallographically characterized.[25–27] Therefore, we undertook single crystal X-ray diffraction studies to discern the solid state structures of **1** and **2**. Table I lists the collection parameters for **1** and **2**. Tables II and III are the heavy atom positional parameters for **1** and **2**, respectively. Table IV is a tabulation of the metrical data for **1** and **2**.

Crystallographic Studies

We are aware of only two other Zr hetero- or homo-alkoxide complexes for which crystal structures have been reported,[25–27] $[Zr(OPr^i)_4(HOPr^i)]_2$[9,15,17]

TABLE I Collection data for $[Zr(\mu\text{-}OCHMe_2)(OCH_2CMe_3)_4(HOCH_2CMe_3)]_2$, **1**, and $[Ta(\mu\text{-}OCH_2Me)(OCH_2CMe_3)_4]_2$, **2**

Compound	**1**	**2**
Chemical formula	$C_{46}H_{102}O_{10}Zr_2$	$C_{44}H_{98}O_{10}Ta_2$
Formula weight	997.72	1149.12
Temperature (K)	198	198
Space group	C2/c	$P\bar{1}$
a (Å)	10.731 (2)	10.246 (1)
b (Å)	26.843 (3)	10.526 (1)
c (Å)	19.733 (2)	14.339 (1)
α (deg)		68.966 (7)
β (deg)	96.77 (1)	71.40 (1)
γ (deg)		82.00 (1)
V (Å^3)	5644 (1)	1367 (1)
Z	4	1
D_{calcd} (Mg/m^3)	1.174	1.395
μ (mm^{-1})	0.415	4.043
$R1$[a] (%)	8.13	3.34
$R1$[a] (%, all data)	14.65	3.88
$R2w$[b] (%, $I > 2\sigma(I)$)	21.11[c]	8.68[d]
$R2w$[b] (all data)	26.06[c]	8.97[d]

[a] $R1 = \sum||F_0| - |F_c||/\sum|F_0| \times 100$.

[b] $R2w = [\sum w(F_0^2 - F_c^2)^2/\sum(w|F_o|^2)^2]^{1/2} \times 100$.

Final weighting scheme calc:

[c] $w = 1/[\alpha^2(F_0^2) + (0.1416P)^2$,

[d] $w = 1/[\alpha^2(F_0^2) + (0.0538P)^2$, where $P = (F_0^2 + 2F_c^2)/3$.

TABLE II Atomic coordinates ($\times 10^5$) for **1**

Atoms	*x*	*y*	*z*	*U*(eq)*
Zr(1)	0	1170 (1)	2500	55 (1)
Zr(2)	0	−133 (1)	2500	49 (1)
O(1)	573 (5)	521 (2)	1975 (3)	42 (2)
O(2)	1716 (6)	12 (2)	3177 (3)	49 (2)
O(3)	1779 (6)	1027 (2)	3125 (3)	47 (2)
O(4)	778 (7)	−601 (3)	1931 (5)	84 (3)
O(5)	593 (7)	1656 (3)	1882 (4)	86 (3)

* U(eq) is defined as one third of the trace of the orthogonalized U_{ij} tensor.

TABLE III Atomic coordinates ($\times 10^5$) for **2**

Atoms	*x*	*y*	*z*	*U*(eq)*
Ta(1)	54 (1)	4290 (1)	1290 (1)	34 (1)
O(1)	1037 (3)	5605 (4)	−228 (3)	35 (1)
O(2)	1105 (5)	2768 (4)	983 (3)	54 (1)
O(3)	−1107 (4)	5732 (4)	1632 (3)	51 (1)
O(4)	−1164 (5)	3011 (5)	2416 (3)	63 (1)
O(5)	1355 (5)	4583 (5)	1874 (4)	59 (1)

* U(eq) is defined as one third of the trace of the orthogonalized U_{ij} tensor.

TABLE IV Selected bond distances (Å) and angles (deg) for **1** and **2**

	1		**2**	
Bond Distance (Å)				
M···M	Zr(1)–Zr(2)	3.498 (2)	Ta(1)–Ta(2)	3.490 (1)
M–OR				
	Zr(1)–O(5)	1.943 (7)	Ta(1)–O(5)	1.893 (4)
	Zr(2)–O(4)	1.939 (7)	Ta(1)–O(4)	1.896 (4)
	Zr(1)–O(3)	2.181 (3)	Ta(1)–O(3)	1.902 (4)
	Zr(2)–O(2)	2.179 (6)	Ta(1)–O(2)	1.908 (4)
M–(μ–OR)				
	Zr(1)–O(1)	2.154 (6)	Ta(1)–O(1)	2.120 (3)
	Zr(2)–O(1)	2.164 (6)	Ta(1)–O(1A)	2.124 (3)
Bond angles (deg)				
M–(μ-OR)–M	Zr(1)–O(1)–Zr(2)	108.2 (2)	Ta(1)–O(1)–Ta(1A)	110.6 (1)
(μ-OR)–M–(μ-OR)	O(1)–Zr(1)–O(1A)	72.0 (3)	O(1)–Ta(1)–O(1A)	69.4 (1)
	O(1)–Zr(2)–O(1A)	71.6 (3)		
(μ-OR)–M–(OR)	O(1)–Zr(1)–O(3)	81.3 (2)	O(1)–Ta(1)–O(2)	90.7 (2)
	O(1)–Zr(1)–O(3A)	82.3 (2)	O(1)–Ta(1)–O(3)	92.0 (2)
	O(1)–Zr(1)–O(5)	96.2 (3)	O(1)–Ta(1)–O(4)	162.0 (2)
	O(1A)–Zr(1)–O(3)	82.3 (2)	O(1)–Ta(1)–O(5)	93.3 (2)
	O(1A)–Zr(1)–O(5)	168.0 (3)	O(1A)–Ta(1)–O(2)	89.3 (2)
			O(1A)–Ta(1)–O(3)	88.7 (2)
			O(1A)–Ta(1)–O(4)	92.8 (2)
			O(1A)–Ta(1)–O(5)	162.7 (2)
(RO)–M–(OR)	O(3)–Zr(1)–O(3)	159.7 (3)	O(2)–Ta(1)–O(3)	175.9 (2)
	O(3)–Zr(1)–O(5)	98.3 (3)	O(2)–Ta(1)–O(4)	86.9 (2)
	O(3A)–Zr(1)–O(5)	95.3 (3)	O(2)–Ta(1)–O(5)	91.7 (2)
	O(5)–Zr(1)–O(5A)	95.6 (6)	O(3)–Ta(1)–O(4)	89.6 (2)
			O(3)–Ta(1)–O(5)	91.2 (2)
			O(4)–Ta(1)–O(5)	104.6 (2)
M–O–C			Ta(1)–O(2)–C(3)	151.0 (4)
	Zr(1)–O(3)–C(5)	130.2 (6)	Ta(1)–O(3)–C(5)	152.1 (4)
	Zr(1)–O(5)–C(9A)	135.4 (1)	Ta(1)–O(4)–C(7)	141.8 (7)
			Ta(1)–O(5)–C(9)	144.3 (6)
M–(μ-O)–C	Zr(1)–O(1)–C(1)	114.0 (1)	Ta(1)–O(1)–C(1)	123.1 (6)
	Zr(1)–O(1)–C(1A)	146 (2)		

and [(μ-THME)Zr_2(OPr^i)$_5$]$_2$.[15] Many other crystal structures of alkoxide containing Zr compounds with alternative supporting ligands have been reported.[28–31] A thermal ellipsoid plot of **1** is shown in Figure 2. The general constructs of **1** are consistent with the homoleptic OPr^i derivative.[9] **1** has a two-fold rotation axis through the Zr atoms and adopts an edge-shared bioctahedral geometry with an assumed coordinated alcohol (for charge balance) per Zr atom. For the OPr^i derivative, the coordinated alcohol was shown to be axially bound.[9] For **1**, there is not sufficient distinction between the various alkoxide M–O distances to definitively assign the coordinated alcohol; moreover, the two-fold symmetry dictates that the

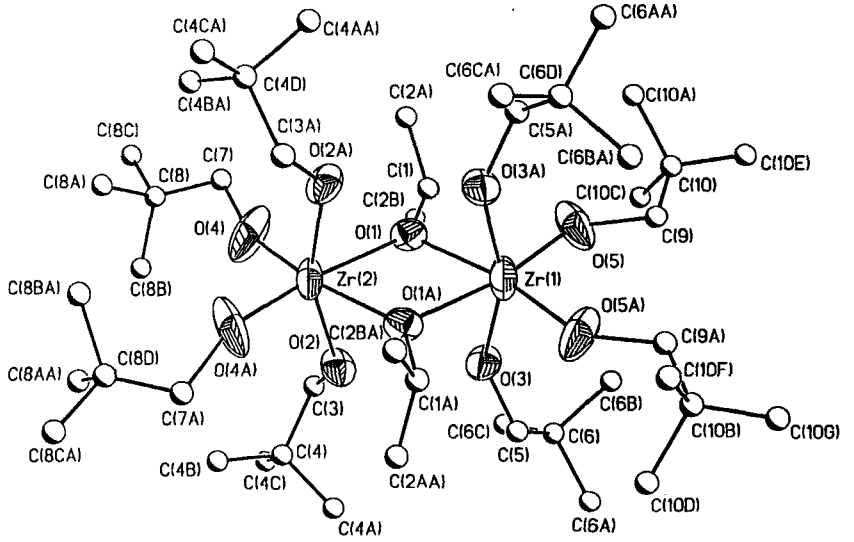

FIGURE 2 Thermal ellipsoid plot of $[Zr(\mu\text{-}OPr^i)(ONp)_3(HONp)]_2$, **1**. Thermal ellipsoids are drawn at the 50% level.

coordinated alcohol is disordered over at least two sites. Due to the lack of evidence for the alcoholic proton in the crystal data, the crystal structure is most likely an ensemble of different conformers with the coordinated alcohol occupying each of the sites equally; however, there are some indications that the HONp is preferentially located in the axial position. H-bonding between the axial alcohol and the axial alkoxide ligand (distance of 2.76–2.78 Å) was observed in the OPr^i derivative.[9] The distance between the axial oxygens of **1** is 2.72 Å, which is even shorter than that observed for the OPr^i derivative. Furthermore, the Zr(2)···Zr(1)–O(3) and the Zr(1)···Zr(2)–O(2) angles are 79.8 (2)° and 79.4 (1)°, respectively, which are comparable with the analogous angle of the OPr^i complex ($Zr'\cdots Zr\text{-}(H)OPr^i$, 79.5°). The remainder of the metrical data for **1** are consistent with those observed for the parent alkoxide derivative, wherein bond distances aggrandized with increased bonding [ave. 2.06 (OR_{term}) < ave. 2.16 (μ-OR)].

A majority of the homoleptic Ta alkoxide derivatives are liquids [i.e., OEt, OBu (OBu = $OCMe_3$), and OEtOMe] prohibiting crystallographic characterization.[8,18,19,32] The OMe and OPr^i derivatives were reported to be edge-shared octahedral dinuclear complexes; however, only the unit cell dimensions were reported.[8,18,19,32] Figure 3 is the thermal ellipsoid plot of **2** which is consistent with the homoleptic ligated complexes.[8,18,19,32] **2** adopts an edge-shared bioctahedral geometry (related by a center of inversion)

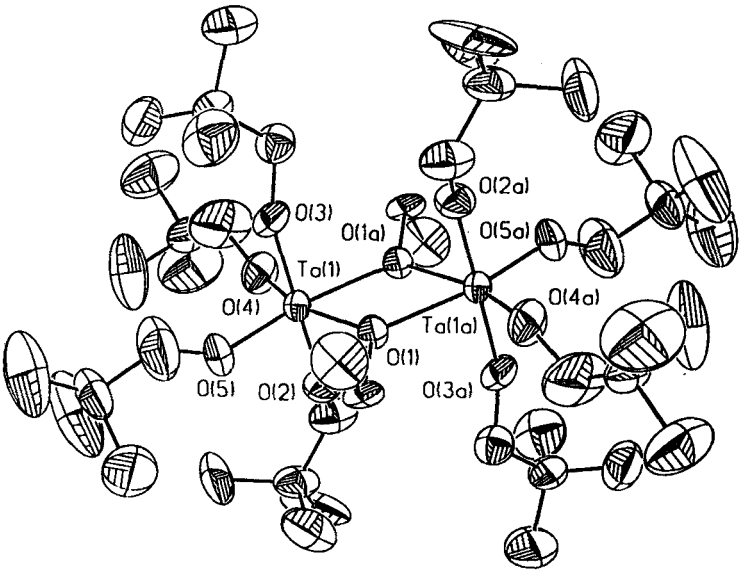

FIGURE 3 Thermal ellipsoid plot of $[Ta(\mu\text{-OEt})(ONP)_4]_2$, **2**. Thermal ellipsoids are drawn at the 50% level.

with the OEt ligands acting as the bridge. This structure is consistent with the *proposed* structure for the less sterically demanding mixed alkoxide of $[Ta(\mu\text{-OMe})(OPr^i)_4]_2$[5] and the reported dinuclear structure determined from X-ray photographs of $[Ta(OMe)(OBu^t)_4]_2$.[16] Since minimal data were reported for the crystallographically characterized $Ta(OR)_5$ complexes, other complexes were used for comparisons. $Ta_2(\mu\text{-O})(\mu\text{-OPr}^i)(OPr^i)_7(HOPr^i)$,[18,19,32] $Ta_7(\mu_3\text{-O})_3(\mu\text{-O})_6(\mu\text{-OPr}^i)_4(OPr^i)_{13}$,[18,19,32] and $[Ta(\mu\text{-OMe})(OMe)_2(2,6\text{-}OC_6H_3(OPr^i)_2)_2]_2$[33] have been fully reported and have similar geometrical arrangements as observed for **2**. The terminal bond distances, ave. 1.90 (1) Å, and bridging bond distances, ave. 2.12 (1) Å, for **2** are consistent with the compounds previously reported. The remaining angles of central core and octahedral metal centers of **2** are consistent with the metrical data reported for the above compounds.

FT-IR

The FT-IR spectra of compounds $[Ti(\mu\text{-ONp})(ONp)_3]_2$, $[Nb(\mu\text{-OEt})(ONp)_4]_2$, **1**, and **2** are very similar due to the dominance of the ONp ligands. For the mixed ligated species ($[Nb(\mu\text{-OEt})(ONp)_4]_2$, **1**, and **2**) the standard stretches reported for the ONp ligand[12,13] are more distorted in

comparison to those of $[Ti(\mu\text{-}ONp)(ONp)_3]_2$, due to the overlap from the OEt or OPr^i ligand stretches. The M–O region (800–600 cm^{-1}) of **1** has sharper stretches than that of the OPr^i derivative. This difference may be due to the number of rotamers noted for the solid state structure of $[Zr(OPr^i)_4(HOPr^i)]_2$.[9] The spectra of $[Nb(\mu\text{-}OEt)(ONp)_4]_2$ and **2** are also almost indistinguishable except in the M–O region: for $[Nb(\mu\text{-}OEt)(ONp)_4]_2$ there is one major stretch at 635 with two minor stretches present at 610 and 592 cm^{-1}: for **2** there is one major stretch at 649 cm^{-1} with two smaller stretches at 685 and 661 cm^{-1}.

Solution State

Compound **1** and $[Zr(OPr^i)_4(HOPr^i)]_2$ adopt similar solid state structures and should, in a general sense, possess similar solution behavior. Since the Group (IV) congener, $[Nb(\mu\text{-}OEt)(ONp)_4]_2$, and **2** adopt similar structures in the solid state, it is assumed that their solution behavior would correlate as well. $[Nb(\mu\text{-}OEt)(ONp)_4]_2$ was found to possess an equilibrium between dinuclear and higher order oligomers.[13] To verify the solution nuclearity and to determine the behavior/nature of **1** and **2**, molecular weight and NMR studies were undertaken (*vide infra*).

Molecular Weight

Bradley reported the molecular complexity (MC) of "$Zr(OPr^i)_4$" (MC = 3.0), "$Zr(ONp)_4$" (MC = 2.4), $[Zr(OPr^i)_4(HOPr^i)]_2$ (MC = 2.0), "$Ta(OEt)_5$" (MC = 1.98) and "Ta(O-*n*-pentyl)$_5$" (MC = 2.01) in boiling benzene.[5] It was observed that $Ta(OR)_5$ complexes have a MC = 2 in boiling benzene and a slightly lower MC at higher temperatures (boiling toluene). Solution molecular weight determinations by the Signer Method[34] were undertaken to determine the nuclearity of **1** and **2** in solution; however, these effects were thwarted by the preferential crystallization of **1** out of toluene or C_6D_6 during equilibration. Other solvents can obviously be used to determine the solution structures of these compounds; however, chlorinated solvents typically cannot be used for materials applications and the use of alcohol solvents will result in ligand exchange. HONp cannot be used since it is a solid. The molecular weight of **2** could not be obtained either, due to the low solubility of this compound in toluene or benzene (as was noted for $[Nb(\mu\text{-}OEt)(ONp)_4]_2$).[13] Further evaluation of the solution behavior of **1** and **2** were undertaken by NMR spectroscopy.

NMR Spectroscopy

Group IV

The solution behavior of the previously characterized $[Zr(OPr^i)_4(HOPr^i)]_2$ was found to be consistent with rapid proton transfer and ligand site exchange and an overly simplistic spectrum was obtained on this compound.[9] VT NMR experiments revealed a large number of resonances at low temperature. It was determined that these were rotamers of the alcoholate and *not* a mononuclear, dinuclear equilibirium,[9] see equation 5.

$$[M(\mu\text{-OR})(OR)_3(HOR)]_2 \rightleftharpoons 2M(OR)_4(HOR) \tag{5}$$

since previous reports on the OPr^i derivative indicated that this compound had a MC = 2.0 in boiling $HOPr^i$.[5] Due to the presence of the alcohol as solvent, little dynamic behavior would be expected.

For **1** there are three types of ligands present, OPr^i, ONp, and HONp. The spectrum of a saturated solution of **1** in C_6D_6 reveals four resonances that correspond to the μ-OPr^i methine (δ 4.73), μ-OPr^i methyl (δ 3.92), ONp methylene (δ 3.92), and ONp methyl (δ 1.08) resonances. This is in agreement with the solid state structure of **1** if there is significant scrambling of the coordinated alcohol's proton among the terminal ONp ligands. A $^{13}C\{^1H\}$ NMR spectrum of this sample revealed five peaks which were consistent with the carbons of the ONp and OPr^i ligands reported for the solid state structure of **1**. It appears, therefore, that the solid state structure of **1** is retained in solution. However, samples at lower concentrations reveal ^1H and ^{13}C NMR spectra that are much more complicated, with the growth of at least 10 new methylene and methyl resonances. Since these NMR spectra are reproducible but vary based upon concentration, an equilibrium must be invoked to account for the observed results.

At low concentrations a mononuclear species should be favored but the simple equilibrium shown in equation (3) for the homoligated species must now be complicated by the introduction of multiple ligands for **1** (Equation (6)). The equilibrium

$$\underbrace{[Zr(\mu\text{-OR}')(OR)_3(HOR)]_2}_{\text{High concentration}} \rightleftharpoons 2Zr(OR')(OR)_3(HOR)$$
$$\rightleftharpoons Zr(OR')_2(OR)_2(HOR) + Zr(OR)_4(HOR) \tag{6}$$

indicates a symmetrical disruption occurred; however, asymmetrical mononuclear compounds would also be expected to form. Furthermore, the presence of room temperature rotamers induced by the steric bulk of the

ONp ligand may also contribute to the complexity of this spectrum. Rotamers were noted for the low temperature spectrum of the OPr^i derivative.[9] The weakly coordinated HONp ligand allows a great deal of dynamic behavior to occur at low concentrations. Therefore, the utility of ^1H and ^{13}C NMR are limited for evaluation of the less than saturated solution behavior of **1**, except for indicating that a large degree of inter- and intraligand exchange occurs.

Surprisingly, a saturated sample of **1** in toluene-d_8 had a spectrum consistent with the C_6D_6 spectrum recorded for the lower concentration samples. It was thought that these spectra could be explained by the lower solubility of **1** in toluene *vs.* benzene.[23] Therefore, a spectrum at 30°C was obtained to increase the amount of material dissolved. The resulting spectrum was consistent with that observed for the saturated C_6D_6 sample. Higher temperatures revealed little further change in the spectrum.

Group V

The dinuclear mononuclear equilibrium behavior (Equation (3)) of "$Ta(OR)_5$" (R = Me, Et, Pr) in solution has been well established by VT NMR experiments and the isolation of Lewis base stabilized monomers.[5] The NMR data collected on $[Nb(\mu\text{-}OEt)(ONp)_4]_2$ also revealed multinuclear exchange, wherein higher order oligomers were present at lower temperatures and monomers formed at elevated temperatures. The multinuclear equilibrium was difficult to observe using ^1H and ^{13}C NMR but easily observed using ^{93}Nb NMR spectroscopy.[13]

The saturated ^1H spectrum of **2** in C_6D_6 revealed two types of OEt ligands [δ 4.66, 4.52 (methylene); 1.46, 1.36 (methyl)] and more than three types of ONp ligands [δ 4.44, 4.42, 4.39 (methylene); 1.77, 1.14, 1.08, 0.86 (methyl)] which is more complex than can be accounted for by the solid state structure. For samples at lower concentrations, only one set of OEt [δ 3.30 (methylene); 0.87 (methyl)] and ONp [δ 3.00 (methylene) and 0.85 (methyl)] resonances were observed. These spectra were reproducible for any given concentration, verifying that an equilibrium exists for **2** in C_6D_6.

If the observed mononuclear/dinuclear equilibrium for "$Ta(OEt)_5$" exists for **2**, the lower concentrations should favor the mononuclear form (Equation 7).

$$\underbrace{2Ta(OR')(OR)_4}_{\text{Low concentration}} \rightleftharpoons [Ta(\mu\text{-}OR')(OR)_4]_2 \rightleftharpoons \tfrac{2}{3}Ta_3(\mu\text{-}OR')_3(OR)_{12} \rightleftharpoons \tfrac{1}{2}Ta_4(\mu\text{-}OR')_4(OR)_{16} \qquad (7)$$

The resonances noted for the less concentrated samples would be consistent with the symmetric division of the heteroligated complex forming "$Ta(OEt)(ONp)_4$". The absence of resonances in this area for the concentrated sample of **2** indicates that the peaks observed for the concentrated samples must be associated with either higher order oligomers (Equation (6)) and/or inter-ligand exchange products. Higher nuclearity products were noted for saturated samples of the Nb analog.[13]

Investigation of the solution behavior of **2** in boiling toluene-d_8 was also undertaken in an attempt to reach the high temperature ligand exchange limit; however, even more complex ^1H and ^{13}C NMR spectra were obtained at both room and high temperature in comparison to the C_6D_6 samples. There was little difference noted for the solubility of **2** in either solvent.[24] Due to the success of using ^{93}Nb NMR to identify complex solution behavior not observable by standard nuclei for $[Nb(\mu\text{-}OEt)(ONp)_4]_2$,[13] ^{91}Ta NMR experiments were undertaken. Unfortunately, these proved fruitless due to the high asymmetry of the resulting *in situ* compounds causing extremely broad peaks.

CONCLUSION

Two novel, mixed-alkoxy, neo-pentoxide Group (IV) and (V) compounds have been synthesized and identified in the solid state as $[Zr(\mu\text{-}OCHMe_2)(OCH_2CMe_3)_3(HOCH_2CMe_3)]_2$ (**1**) and $[Ta(\mu\text{-}OCH_2Me)(OCH_2CMe_3)_4]_2$ (**2**). For each, an incomplete alcoholysis exchange was noted for the alcoholysis exchange route. The remaining parent (OPr^i and OEt) alkoxide ligands act as the bridging moieties of the central core. Since the parent alkoxides are reportedly dinuclear in the solid and solution state and only the terminal alkoxides were exchanged, the central core of the parent alkoxides were not significantly disrupted during the synthesis of **1** or **2**.

The ^1H and ^{13}C NMR spectra obtained for **1** and **2** proved to be very complex. NMR studies revealed that the solid state structure was retained for *saturated* solutions of **1**; however, less concentrated samples indicated that a great deal of intra- and inter-molecular exchange occurred. The complicated spectra of **1** are associated with the weakly coordinated HONp ligand and the preferential solubility in benzene *vs.* toluene.[23] The homoleptic $[Zr(OPr^i)_4(HOPr^i)]_2$ analog has a simplified spectrum due to reduced stability of mononuclear species and a single ligand type. The NMR spectra of concentrated samples of **2** revealed that an equilibrium exists between

the dinuclear and higher nuclearity species, as was previously noted for the $[Nb(\mu\text{-}OEt)(ONp)_4]_2$.[13] NMR spectra of low concentration samples of **2** revealed that only one compound was present in solution; this compound has been tentatively assigned as the mononuclear "$Ta(OEt)(ONp)_4$" species. At high concentrations, a complex multi-equilibrium was noted at room temperature. A sufficiently high temperature could not be achieved to demonstrate an NMR spectrum associated solely with the dinuclear solid state compound.

These mixed dinuclear species adopt "simple" solid state structures but demonstrate very complex behavior. The two types of alkoxides present in these hetero-alkoxide species, combined with the steric stability of the ONp ligand, allow for a wide number of compounds to exist simultaneously in solution, in contrast to the homoleptic parent alkoxides. The ease of generation of the mixed-ligands species indicates that sterically controlled precursors can be designed for specific applications.

Supporting Information Available

A complete listing of crystal data collection, positional and thermal parameters, bond distances and angles and addition figures for **1** and **2** (21 pp.) are available.

Acknowledgments

This work supported by the United States Department of Energy under contract number DE-AC04-94AL85000. Sandia is a multiprogram laboratory operated by Sandia Corporation, a Lockheed Martin Company, for the United States Department of Energy. The authors would also like to thank Dr. T.M. Alam for assistance in the NMR investigations.

References

[1] L.G. Hubert-Pfalzgraf, *New. J. Chem.* **11**, 663 (1987).
[2] K.G. Caulton and L.G. Hubert-Pfalzgraf, *Chem. Rev.* **90**, 969 (1990).
[3] C.D. Chandler, C. Roger and M.J. Hampden-Smith, *Chem. Rev.* **93**, 1205 (1993).
[4] D.C. Bradley *Chem. Rev.* **89**, 1317 (1989).
[5] D.C. Bradley, R.C. Mehrotra and D.P. Gaur, *Metal Alkoxides*, Academic Press: New York, 1978.
[6] T.J. Boyle, H.N. Al-Shareef, C.D. Buchheit, R.T. Cygan, D. Dimos, M.A. Rodriguez, B. Scott and J.W. Ziller, *Integrated Ferroelectrics* **18**, 213 (1997).
[7] T.J. Boyle and H.N. Al-Shareef, *J. Mater. Sci.* **32**, 2263 (1997).
[8] A.I. Yanovskii, E.P. Turesvskaya, N.Y. Turova, F.M. Dolgushin, A.P. Pisarevskii, A.S. Batsanov and Y.T. Struchkov, *Russ. J. Inorg. Chem.* **39**, 1246 (1994).
[9] B.A. Vaartstra, J.C. Huffman, P.S. Gradeff, L.G. Hubert-Pfalzgraf, J.-C. Daran, S. Parraud, K. Yunlu and K.G. Caulton, *Inorg. Chem.* **29**, 3126 (1990).

[10] D.A. Wright and D.A. Williams, *Acta Crystallogr., Sect. B* **24**, 1107 (1968).
[11] J.A. Ibers, *Nature (London)* **197**, 686 (1963).
[12] T.J. Boyle, T.M. Alam, E.R. Mechenbeir, B. Scott and J.W. Ziller, *Inorg. Chem.* **36**, 3293 (1997).
[13] T.J. Boyle, T.A. Alam, D. Dimos, G.J. Moore, C.D. Buchheit, H.N. Al-Shareef, E.R. Mechenbier and B.R. Bear, *Chem. Mater.* **9**, 3187 (1997).
[14] A.A. Pinkerton, D. Schwarzenbach, L.G. Hubert-Pfalzgraf and J.G. Reiss, *Inorg. Chem* **15**, 1196 (1976).
[15] T.J. Boyle, R.W. Schwartz, R.J. Doedens and J.W. Ziller, *Inorg. Chem.* **34**, 1110 (1995).
[16] N.A. Imam and B.R. Rao, *Naturwissensehaften* **51**, 263 (1964).
[17] S.A. Imam and B.R. Rao, *Naturwissenschaften* **50**, 517 (1963).
[18] A.I. Yanovsky, N. Ya, N.Y. Turova, A.V. Korolev, D.E. Chebukov, A.P. Pisarevsky and Y.T. Struchkov, *Izv. Akad. Nauk SSSR, Ser. Khim.* 125 (1996).
[19] A.I. Yanovsky, E.P. Turevskaya, N.Y. Turova, A.P. Dolgushin, A.P. Pisarevsky and A.S. Batsano, *Zh. Neorg. Khim.* **39**, 1307 (1994).
[20] XSCANS and SHELXTL PC are products of Siemens Analytical X-ray Instruments, Inc., 6300 Enterprise Lane, Madison, Wisconsin 53719. SHELX-93 is a program for crystal structure refinement written by G.M. Sheldrick (1993), Univ. of Gottingen, Germany.
[21] T.J. Boyle, D.M. Pedrotty, B. Scott and J.W. Ziller, *Polyhedron* **17**, 1959 (1998).
[22] T.J. Boyle, D.C. Bradley, M.J. Hampden-Smith, A. Patel and J.W. Ziller, *Inorg. Chem.* **34**, 5893 (1995).
[23] A 0.050 M solution of **1** could be produced in C_6D_6; however, only a 0.036 M solution of **1** could be produced in toluene.
[24] A 0.0145 M or 0.0140 M solution of **2** in C_6D_6 or toluene, respectively, could be generated.
[25] The Cambridge Structural Database was used for determination of structure types, literature references, bond distances, and bond angles.
[26] F.H. Allen, S. Bellard, M.D. Brice, B.A. Cartwright, A. Doubleday, H. Higgs, T. Hummelink, B.G. Hummelink-Peters, O. Kennard, W.D.D. Motherwell, J.R. Rodgers and D.G. Watson, *Acta Crystallogr.* **B35**, 146 (1979).
[27] F.H. Allen, O. Kennard and R. Taylor, *Acc. Chem. Res.* **16**, 146 (1983).
[28] Examples of other 6 oxygen-coordinated Zr complexes found in the CDB are cited in Refs. [29–31].
[29] J.A. Samuels, E.B. Lobkovsky, W.E. Streib, K. Folting, J.C. Huffman, J.W. Zwanziger and K.G. Caluton, *J. Am. Chem. Soc.* **115**, 5093 (1993).
[30] P. Toledano, M. In and C. Sanchez, *C.R. Seances Acad. Sci. Ser. 2*, **311**, 1161 (1990).
[31] B. Morosin, *Acta Cryst., Sect B.* **1977**, 303 (1977).
[32] N.Y. Turova, A.V. Korolev, D.E. Tchebukov, A.I. Belokon, A.I. Yanovsky and Y.T. Struchkov, *Polyhedron* **15**, 3869 (1996).
[33] R. Wang, K. Folting, J.C. Huffman, L.R. Chamberlain and I.P. Rothwell, *Inorg. Chim. Acta* **120**, 81 (1986).
[34] E.P. Clark, *Analytical Ed.* 820 (1941).